Screening in $(d+s)$-wave superconductors: Application to Raman scattering

Andreas P. Schnyder and Christopher Mudry

Condensed Matter Theory Group, Paul Scherrer Institute, CH-5232 Villigen PSI, Switzerland

Dirk Manske

Institut für Theoretische Physik, ETH Zürich, Hönggerberg, CH-8093 Zürich, Switzerland and
Max-Planck-Institut für Festkörperforschung, D-70569 Stuttgart, Germany
(Dated: February 6, 2008)

We study the polarization-dependent electronic Raman response of untwinned $YBa_2Cu_3O_{7-\delta}$ superconductors employing a tight-binding band structure with anisotropic hopping matrix parameters and a superconducting gap with a mixing of d- and s-wave symmetries. Using general arguments we find screening terms in the B_{1g} scattering channel which are required by gauge invariance. As a result, we obtain a small but measurable *softening* of the pair-breaking peak, whose position has been attributed for a long time to twice the superconducting gap maximum. Furthermore, we predict superconductivity-induced changes in the phonon line shapes that could provide a way to detect the isotropic s-wave admixture to the superconducting gap.

I. INTRODUCTION

The symmetry of the superconducting (SC) order parameter in cuprate high-T_c superconductors is now agreed to be unconventional after early intense theoretical and experimental debates.[1] Phase-sensitive experiments such as corner-junction superconducting quantum interference device experiments [2] and tricrystal experiments on $YBa_2Cu_3O_{7-\delta}$ (YBCO) (Ref. [3]) show that the SC order parameter undergoes sign changes in the Brillouin zone (BZ) that are consistent with the $d_{x^2-y^2}$ symmetry. A sign change of a SC order parameter with the $d_{x^2-y^2}$ symmetry implies the existence of four nodal points in the Brillouin zone that have been observed using momentum-resolved probes such as inelastic neutron scattering (INS) or angle-resolved photoemission spectroscopy (ARPES). Correspondingly, the simple gap

$$\Delta_{\boldsymbol{k}} = \Delta_0(\cos k_x - \cos k_y)/2 \qquad (1.1)$$

with a $d_{x^2-y^2}$ symmetry on the Brillouin zone has often been used as a starting point of a quantitative interpretation of these experiments.

Of course, a sign change in the SC gap does not preclude a gap that is more complicated than the simple $d_{x^2-y^2}$ gap (1.1). For those high-T_c cuprates with a tetragonal crystalline structure, higher d-wave harmonics have been invoked to explain ARPES measurements of the magnitude of the SC gap.[4] For the cuprate family $YBa_2Cu_3O_{7-\delta}$, which exhibits quite strong orthorhombic distortions, one expects corrections to the $d_{x^2-y^2}$ gap (1.1) on symmetry grounds alone. This expectation has been confirmed by several experimental methods such as ARPES studies,[5] INS studies,[6] and measurements of Josephson currents,[7, 8] and has also been investigated theoretically.[9, 10, 11]

Polarization-dependent electronic Raman scattering also probes the momentum dependence of the magnitude of the superconducting order parameter and has provided yet one more piece of evidence for the $d_{x^2-y^2}$-wave pairing scenario.[12, 13, 14] In particular, for tetragonal high-T_c cuprates, one finds (a) various low-energy power laws in different polarization channels that are consistent with the existence of nodal points for the gap and (b) the pair-breaking peak in the B_{1g} channel at energy twice the superconducting gap maximum $\widetilde{\Delta}_0$ seen by other means.[15]

In this paper, we are going to investigate the consequences for polarization-dependent Raman scattering of a subdominant admixture of an isotropic s-wave component to the gap (1.1) which should be of relevance to orthorhombic high-T_c superconductors of the YBCO family. Assuming the existence of well-defined SC quasiparticles, we compute the polarization-dependent electronic Raman-scattering cross section including the effects of (i) an orthorhombic tight-binding dispersion with $(d+s)$ gap, (ii) a long-range Coulomb interaction treated within the random-phase approximation (RPA), (iii) and the effective mass approximation for the Raman vertex. We show that the pair-breaking peak in the B_{1g} channel is softened by an amount proportional to the isotropic s component to the gap in that it occurs at a lower value than the absolute maximum of the gap on the "normal-state" Fermi surface. We also show that the A_{1g} channel develops a double peak structure with the peak separation proportional to the isotropic s component to the gap. Furthermore, we compute superconductivity-induced changes in the phonon line shapes, and argue how Raman scattering on phonons allows us to extract a signature of a subdominant and isotropic s-wave component to the gap.

II. THEORY

The differential cross section in a Raman-scattering experiment for a momentum transfer $\boldsymbol{q}$ that is small compared to the extension of the Brillouin zone is proportional to $[1 + n(\omega)]\chi''_\gamma(\omega)$, where n denotes the Bose distribution, ω the frequency of the incoming plane wave, and

$$\chi_\gamma(\omega) = \left(\chi'_\gamma + i\chi''_\gamma\right)(\omega) \equiv \chi_\gamma(\boldsymbol{q} \approx 0, \omega + i\eta) \quad (2.1a)$$

is the linear-response function for the density operator

$$\rho_{\boldsymbol{q}} = \sum_{\boldsymbol{k}} \sum_{\sigma=\uparrow,\downarrow} \gamma_{\boldsymbol{k}} c^\dagger_{\boldsymbol{k}+\boldsymbol{q},\sigma} c_{\boldsymbol{k},\sigma}. \qquad (2.1b)$$

The coupling between the SC quasiparticles, linear superpositions of the fermionic creation $c_{\boldsymbol{k},\sigma}^\dagger$ and annihilation $c_{\boldsymbol{k},\sigma}$ operators, and the incoming (outgoing) plane wave with the polarization vector $\hat{e}^I$ ($\hat{e}^O$) is here approximated by

$$\gamma_{\boldsymbol{k}} \propto \sum_{\alpha,\beta} \hat{e}_\alpha^O \frac{\partial^2 \varepsilon_{\boldsymbol{k}}}{\partial k_\alpha \partial k_\beta} \hat{e}_\beta^I \qquad (2.1c)$$

in the nonresonant limit. The "normal-state" dispersion

$$\begin{aligned}
\varepsilon_{\boldsymbol{k}} =\ & -2t\left[(1+\delta_0)\cos k_x + (1-\delta_0)\cos k_y\right] \\
& -4t'\cos k_x \cos k_y - \mu
\end{aligned} \qquad (2.1d)$$

(see Figs. 1 and 2 in Ref. 16) combines with the gap

$$\Delta_{\boldsymbol{k}} = \frac{\Delta_0}{2}\left(\cos k_x - \cos k_y\right) + \Delta_s \qquad (2.1e)$$

to give the SC quasiparticle dispersion $E_{\boldsymbol{k}} = \sqrt{\varepsilon_{\boldsymbol{k}}^2 + \Delta_{\boldsymbol{k}}^2}$. Both δ_0 and Δ_s represent symmetry-breaking terms that lower the symmetry from tetragonal to orthorhombic in an effective one-band description of a single copper-oxygen plane. The s-wave component Δ_s is isotropic [compared with the extended s-wave admixture from Eq. (3.8)]. The Raman vertices $\gamma_{\boldsymbol{k}}$ can be classified according to the irreducible representations of the symmetry group of the crystal. For a crystal with tetragonal symmetry (point group D_{4h}), the relevant symmetries are the B_{1g}, B_{2g}, and A_{1g} polarizations. As we shall consider a model with subdominant orthorhombic distortions, $\delta_0 \ll 1$, $\Delta_s \ll \Delta_0$, we will use, in what follows, the notation of tetragonal symmetry.[17] If so, we can identify the B_{1g}, B_{2g}, and A_{1g} channels for Raman scattering with the Raman vertices

$$\gamma_{B_{1g}\,\boldsymbol{k}} \propto t\left[(1+\delta_0)\cos k_x - (1-\delta_0)\cos k_y\right], \quad (2.2a)$$

$$\gamma_{B_{2g}\,\boldsymbol{k}} \propto 4t'\sin k_x \sin k_y, \qquad (2.2b)$$

$$\begin{aligned}
\gamma_{A_{1g}\,\boldsymbol{k}} \propto\ & t\left[(1+\delta_0)\cos k_x + (1-\delta_0)\cos k_y\right] \\
& +4t'\cos k_x \cos k_y,
\end{aligned} \qquad (2.2c)$$

respectively.

The electronic Raman response is calculated in the gauge invariant form assuming that the quasiparticles interact through the long-range Coulomb potential $V_{\boldsymbol{q}} = \frac{4\pi e^2}{q^2}$. For the tetragonal symmetry, the RPA for the polarization-dependent Raman response function $\chi_\gamma(\omega)$ was derived in Refs. 15, 18 and 14, 19, 20, 21 and shown to be well defined in the limit $\boldsymbol{q} \to 0$.

Its generalization to orthorhombic symmetry leads to

$$\chi_{B_{1g}}(\omega) = \left\langle \gamma_{B_{1g}}^2 \theta_{\boldsymbol{k}} \right\rangle_\omega - \frac{\left\langle \gamma_{B_{1g}} \theta_{\boldsymbol{k}} \right\rangle_\omega^2}{\langle \theta_{\boldsymbol{k}} \rangle_\omega}, \qquad (2.3a)$$

$$\chi_{B_{2g}}(\omega) = \left\langle \gamma_{B_{2g}}^2 \theta_{\boldsymbol{k}} \right\rangle_\omega, \qquad (2.3b)$$

$$\chi_{A_{1g}}(\omega) = \left\langle \gamma_{A_{1g}}^2 \theta_{\boldsymbol{k}} \right\rangle_\omega - \frac{\left\langle \gamma_{A_{1g}} \theta_{\boldsymbol{k}} \right\rangle_\omega^2}{\langle \theta_{\boldsymbol{k}} \rangle_\omega}, \qquad (2.3c)$$
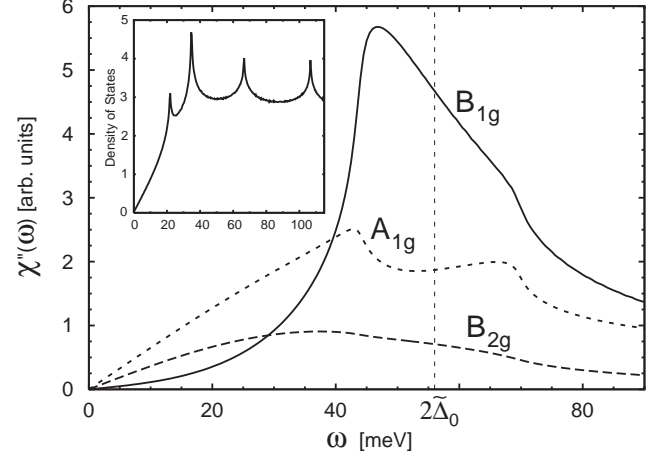

FIG. 1: Calculated electronic Raman response of $(d+s)$-wave superconductors for the B_{1g}, B_{2g}, and A_{1g} channels (tetragonal notation), respectively, according to Eq. (2.3). The B_{1g} pair-breaking peak softens to $\omega \simeq 44$meV $< 2\widetilde{\Delta}_0 \simeq 56$meV where $\widetilde{\Delta}_0$ is the SC gap maximum on the FS defined in Eq. (3.1). The A_{1g} spectrum has been multiplied by the factor of 20. Inset: "bare" density of states in the superconducting state for orthorhombic symmetry.

in the B_{1g}, B_{2g}, and A_{1g} channels for Raman scattering, respectively. As usual, the bracket (in a box of volume V)

$$\begin{aligned}
\langle(\cdots)\theta_{\boldsymbol{k}}\rangle_\omega =\ & \frac{1}{V}\sum_{\boldsymbol{k}}(\cdots)\Delta_{\boldsymbol{k}}^2 \tanh\left(\frac{E_{\boldsymbol{k}}}{2T}\right) \\
& \times \left(\frac{1/E_{\boldsymbol{k}}^2}{\omega+i\eta+2E_{\boldsymbol{k}}} - \frac{1/E_{\boldsymbol{k}}^2}{\omega+i\eta-2E_{\boldsymbol{k}}}\right)
\end{aligned} \qquad (2.4)$$

denotes an average over the BZ weighted by the Tsuneto function $\theta_{\boldsymbol{k}}$.[22] The second term in Eqs. (2.3a) and (2.3c) is commonly called screening term. It can be viewed as originating from the Goldstone mode of the superconductor and ensures gauge invariance of the Raman response.[15] For tetragonal symmetry only screening terms in the A_{1g} scattering channel are possible. That is, the screening term in Eq. (2.3a) is vanishing identically if the SC quasiparticle dispersion is of the tetragonal symmetry. In the presence of orthorhombic distortions of the YBCO type screening terms can affect the B_{1g} channels on general symmetry grounds, but are absent in the B_{2g} channel. Similarly, in orthorhombic $Bi_2Sr_2CaCu_2O_{8+x}$, whose crystallographic axes are rotated by $45°$ with respect to the CuO bonds, screening terms arise in the B_{2g} channel, but do not affect the B_{1g} channel. In the following we shall only consider orthorhombic superconductors of the YBCO type and disregard any possible screening terms in the B_{2g} channel. The presence of screening terms in the B_{1g} or B_{2g} channels for orthorhombic superconductors has been previously reported in the literature, see Refs. 10 and 21.

III. DISCUSSION

We have computed numerically the Raman response (2.3) using the parameters $t = 200$ meV, $\delta_0 = -0.03$, $t'/t = -0.4$,

$\mu/t = -1.2$, $\Delta_0 = 30$ meV, and $\Delta_s = 6$ meV. We also choose the damping $\eta = 1$ meV. This choice yields a SC quasiparticle dispersion that is in qualitative agreement with the one measured by photoemission experiments on un-twinned YBCO close to optimal doping.[23]

In Fig. 1 we show the resulting Raman response for $(d+s)$-wave superconductors. We find that the low-energy asymptotics, $\chi''_{B_{1g}}(\omega) \propto \left(\omega/2\widetilde{\Delta}_0\right)^3$, $\chi''_{B_{2g}}(\omega) \propto \left(\omega/2\widetilde{\Delta}_0\right)$, and $\chi''_{A_{1g}}(\omega) \propto \left(\omega/2\widetilde{\Delta}_0\right)$, remain essentially unchanged with or without the symmetry-breaking terms δ_0 and Δ_s. Here we have introduced the absolute maximum

$$\widetilde{\Delta}_0 = \max_{\boldsymbol{k}\in\text{FS}} \Delta(\boldsymbol{k}) \simeq 28\,\text{meV} \tag{3.1}$$

of the gap over the "normal-state" Fermi surface (FS) with full tetragonal symmetry ($\delta_0 = \Delta_s = 0$). We also find that the relative peak heights in the B_{1g} and A_{1g} responses remain [15] after switching on $\delta_0 > 0$ and $\Delta_s > 0$. These properties are robust to the lowering of the tetragonal to the orthorhombic symmetry as they owe their existence to that of the nodes of the SC gap. There are nevertheless important changes in the line shapes of the A_{1g} and B_{1g} responses due to orthorhombicity which reflect the change in the underlying density of states (see inset of Fig. 1). Most importantly, the B_{1g} pair-breaking peak is not located any longer at the absolute gap maximum $\omega = 2\widetilde{\Delta}_0 \simeq 56$ meV. Instead, it is shifted by $\simeq 2\Delta_s$ to a lower value due to the additional screening term in Eq. (2.3a) and thus its position tracks the position of the double peaks in the A_{1g} channel.[24] This is interesting because it demonstrates that the common lore that the B_{1g} pair-breaking peak is always at $\omega = 2\widetilde{\Delta}_0$ is not correct in $(d+s)$-wave superconductors. In passing, we note that a comparison between the (XX)-polarization channel, $\hat{e}^O = \hat{e}^I = \binom{1}{0}$, and (YY)-polarization channel, $\hat{e}^O = \hat{e}^I = \binom{0}{1}$, reveals only minor differences in the peak positions and line shapes (not shown).

Recently, it has been proposed that vertex corrections to the Raman response function due to a spin-mediated pairing interaction can lead to the development of a resonance below $2\widetilde{\Delta}_0$.[25, 26, 27, 28] Inclusion of these interaction effects would lead to an additional shift of the B_{1g} pair-breaking peak to lower frequencies. However, the magnitude of this shift depends on model assumptions and it remains an open question, whether these vertex corrections are of any relevance for the interpretation of the Raman data on high-T_c cuprates.

In order to analyze in more detail the softening of the B_{1g} pair-breaking peak due to the screening term, we show in Fig. 2 the results for $\Delta_s = 0$ meV, 3 meV, and 6 meV, respectively, with all other parameters held fixed. We find that increasing Δ_s induces a reduction of the peak intensity and a shift to lower frequencies of the peak positions. A closer inspection of Eq. (2.3a) reveals that the bare contribution

$$B^0_{1g}(\omega) = \text{Im}\left\langle \gamma^2_{B_{1g}} \theta_{\boldsymbol{k}}\right\rangle_\omega \tag{3.2}$$

exhibits two peaks located at $\omega = 2(\widetilde{\Delta}_0 \mp \Delta_s)$, respectively. This double peak structure is a reflection of the bare quasiparticle density of states that features two local maxima (inset of
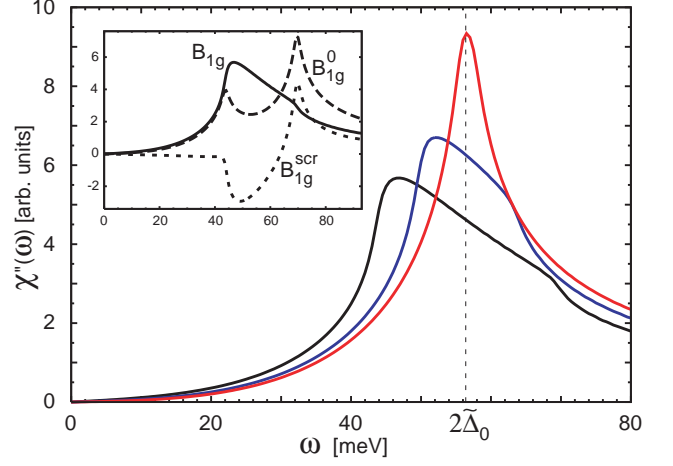

FIG. 2: (color online) Calculated electronic Raman response of $(d+s)$-wave superconductors for the B_{1g} channel (tetragonal notation) according to Eq. (2.3). The fermiology parameters from Eq. (2.1) are the same as in Fig. 1 except for $\Delta_s = 0$ meV (red), $\Delta_s = 3$ meV (blue), and $\Delta_s = 6$ meV (black). Inset: decomposition of the left-hand side of Eq. (2.3a) into the sum of the bare contribution B^0_{1g} and the screening contribution B^{scr}_{1g} on the right-hand side of Eq. (2.3a) when $\Delta_s = 6$ meV.

Fig. 1) at half the frequencies of the peaks in B^0_{1g}. In contrast, the screening contribution

$$B^{\text{scr}}_{1g}(\omega) = \text{Im}\left[\left\langle \gamma_{B_{1g}}\theta_{\boldsymbol{k}}\right\rangle^2_\omega / \left\langle\theta_{\boldsymbol{k}}\right\rangle_\omega\right], \tag{3.3}$$

shows a broad dip followed by a peak (see the inset of Fig. 2). That is, an enhancement of the scattering efficiency by screening (*antiscreening*) occurs at low frequencies $\omega \lesssim 2\widetilde{\Delta}_0$, whereas at high frequencies $\omega \gtrsim 2\widetilde{\Delta}_0$ the scattering efficiency is reduced by the screening term. To show how antiscreening arises, we rewrite the imaginary part of the B_{1g} screening term as

$$B^{\text{scr}}_{1g}(\omega) = \frac{2\left\langle\theta'_{\boldsymbol{k}}\right\rangle_\omega \left\langle\gamma_{B_{1g}}\theta'_{\boldsymbol{k}}\right\rangle_\omega \left\langle\gamma_{B_{1g}}\theta''_{\boldsymbol{k}}\right\rangle_\omega}{\left\langle\theta'_{\boldsymbol{k}}\right\rangle^2_\omega + \left\langle\theta''_{\boldsymbol{k}}\right\rangle^2_\omega} \tag{3.4}$$
$$+ \frac{\left\langle\theta''_{\boldsymbol{k}}\right\rangle_\omega\left[\left\langle\gamma_{B_{1g}}\theta''_{\boldsymbol{k}}\right\rangle^2_\omega - \left\langle\gamma_{B_{1g}}\theta'_{\boldsymbol{k}}\right\rangle^2_\omega\right]}{\left\langle\theta'_{\boldsymbol{k}}\right\rangle^2_\omega + \left\langle\theta''_{\boldsymbol{k}}\right\rangle^2_\omega},$$

where the real and imaginary parts of the Tsuneto functions are denoted by $\theta'_{\boldsymbol{k}}$ and $\theta''_{\boldsymbol{k}}$, respectively. It is instructive to approximate the quasiparticle dispersion by

$$E^2_{k,\phi} \simeq \varepsilon^2_k + |\Delta_\phi|^2 \tag{3.5a}$$

with the linearized dispersion $\varepsilon_k = v_F(k - k_F)$ and the gap function $\Delta_\phi = \widetilde{\Delta}_0\cos(2\phi) + \Delta_s$ that depends only on the Fermi surface angle ϕ. Similarly, we replace the B_{1g} vertex by its angular-dependent form,

$$\gamma_{B_{1g}} \simeq \cos(2\phi). \tag{3.5b}$$

With these simplifications and in the zero-temperature limit the imaginary part of the BZ averages reduce to

$$\langle (\cdots) \theta''_{\boldsymbol{k}} \rangle \simeq \int \frac{k\,dk}{2\pi} \int \frac{d\phi}{2\pi} (\cdots) \frac{\Delta_\phi^2}{E_{k,\phi}^2} \delta\left(\omega - 2E_{k,\phi}\right)$$

$$\simeq \int_{-\delta k}^{+\delta k} \frac{d\tilde{k}}{2\pi} \sum_{\phi_i} (\cdots) \frac{\tilde{k}+k_F}{2E_{\tilde{k}+k_F,\phi_i}} \frac{|\Delta_{\phi_i}|}{|\Delta'_{\phi_i}|}, \quad (3.6)$$

where we have restricted the BZ integration to a ring $-\delta k < k - k_F < \delta k$ around the Fermi surface, the summation runs over all $\phi_i \in \left\{\phi \mid \omega = 2E_{k,\phi}\right\}$, and Δ'_ϕ denotes the derivative of the gap function Δ_ϕ. The imaginary part of the averaged Tsuneto function $\langle \theta''_{\boldsymbol{k}} \rangle$ is a positive function of ω and exhibits a positive divergence whenever $\Delta'_{\phi_i} = 0$, i.e., at the frequencies

$$\begin{aligned} \omega_c^{(1)} &\simeq E_{k_F, \frac{\pi}{2}} = 2(\widetilde{\Delta}_0 - \Delta_s), \\ \omega_c^{(2)} &\simeq E_{k_F, 0} = 2(\widetilde{\Delta}_0 + \Delta_s), \end{aligned} \quad (3.7)$$

as can be seen from the last line of Eq. (3.6). On the other hand, $\langle \gamma_{B_{1g}} \theta'' \rangle$ possesses a negative divergence at $\omega_c^{(1)}$ and a positive divergence at $\omega_c^{(2)}$, and changes its sign at $\sim 2\widetilde{\Delta}_0$, since the B_{1g} vertex $\gamma_{B_{1G}} \simeq \cos 2\phi$ exhibits a sign change along the Fermi surface. Any divergence in the frequency dependence of $\langle \theta'' \rangle$ and $\langle \gamma_{B_{1g}} \theta'' \rangle$ results in a steplike discontinuity in $\langle \theta' \rangle$ and $\langle \gamma_{B_{1g}} \theta' \rangle$, respectively, due to the Kramers-Kronig relation. Vice versa, from the absence of any steplike discontinuity in the imaginary part of the BZ averages follows the absence of any divergence in the real part of the corresponding quantity. Furthermore, it turns out that both $\langle \theta' \rangle$ and $\langle \gamma_{B_{1g}} \theta' \rangle$ are positive in the frequency range $0 \leq \omega \lesssim 2(\widetilde{\Delta}_0 + \Delta_s)$. Taking all these observations together, we find that the first term in the B_{1g} screening function (3.4) features a negative divergence at $\omega = 2(\widetilde{\Delta}_0 - \Delta_s)$, which is compensated by a positive divergence of the second term. But then, at $\omega = 2(\widetilde{\Delta}_0 + \Delta_s)$ both terms in Eq. (3.4) show a positive divergence, which results in a strong screening of the second peak in B_{1g}^0. At $\omega \simeq 2\widetilde{\Delta}_0$ the first term in Eq. (3.4) is vanishing, whereas the second term is negative, which yields to antiscreening of the B_{1g} scattering efficiency.

It is important to note that the effects induced by a nonvanishing isotropic s-wave gap Δ_s in Fig. 2 would not occur had we assumed a subdominant extended s-wave gap such as

$$\begin{aligned} \Delta_{\boldsymbol{k}} &= \Delta_0 \left(\cos k_x - \cos k_y\right)/2 \\ &+ \Delta_s^{\text{ext}} \left(\cos k_x + \cos k_y\right)/2. \end{aligned} \quad (3.8)$$

Contrary to the isotropic subdominant s-wave admixture Δ_s in Eq. (2.1e), the extended s-wave admixture in Eq. (3.8) only leads to a shift of the nodal line, but does not give a different absolute gap value at $(\pi, 0)$ compared to $(0, \pi)$ (see Fig. 2(d) in Ref. 16). From the above discussion one infers that the property $|\Delta_{\phi=\frac{\pi}{2}}| \neq |\Delta_{\phi=0}|$ is crucial for the splitting of the

B_{1g} pair-breaking peak as well as for the appearance of antiscreening in the B_{1g} channel. Thus, we conclude that to a first approximation an extended s-wave admixture leaves the B_{1g} response unchanged, an expectation that we have confirmed by numerical calculations.

IV. SUPERCONDUCTIVITY-INDUCED CHANGES IN PHONON LINE SHAPES

In principle, the existence of a subdominant and isotropic s-wave component Δ_s to the d-wave SC gap can be extracted from a line-shape analysis of the A_{1g} and B_{1g} electronic responses in a polarization-resolved Raman-scattering experiment. However, as part of the electronic Raman signal is in general masked by phonon excitations, it might be hard to detect experimentally these changes in the line shape. On the other hand, we argue in the following that polarization-resolved Raman scattering on phonons can be used to extract a signature of Δ_s.

To substantiate this point, we calculate the superconductivity-induced changes in the self-energy of optical, zone-center ($\boldsymbol{q} = 0$) phonons. Thereto, we consider a linear coupling between electrons and phonons

$$H_{\text{el-ph}} = \frac{1}{V} \sum_{\boldsymbol{k},\boldsymbol{q},\gamma,\sigma} g_{\boldsymbol{k},\boldsymbol{q}}^\gamma c_{\boldsymbol{k}+\boldsymbol{q},\sigma}^\dagger c_{\boldsymbol{k},\sigma} \left(b_{\boldsymbol{q},\gamma} + b_{-\boldsymbol{q},\gamma}^\dagger\right), \quad (4.1)$$

where $b_{\boldsymbol{q},\gamma}^\dagger$ and $b_{\boldsymbol{q},\gamma}$ are the creation and annihilation operators of phonons in a given branch γ with phonon frequency ω_γ, respectively, and $g_{\boldsymbol{k},\boldsymbol{q}}^\gamma$ denotes the electron-phonon coupling. The form of the electron-phonon interaction (4.1) is the one for the nonresonant electronic Raman scattering provided the effective Raman vertex is replaced by the electron-phonon vertex $g_{\boldsymbol{k},\boldsymbol{q}}^\gamma$. Hence, within an RPA treatment of the Coulomb interactions, we find that in the $\boldsymbol{q} \to 0$ limit the superconductivity-induced changes in the phonon self-energy are given by [29, 30, 31]

$$\Sigma_\gamma(\omega) = -\left\langle \left(g_{\boldsymbol{k},0}^\gamma\right)^2 \theta_{\boldsymbol{k}} \right\rangle_\omega + \frac{\left\langle g_{\boldsymbol{k},0}^\gamma \theta_{\boldsymbol{k}} \right\rangle_\omega^2}{\left\langle \theta_{\boldsymbol{k}} \right\rangle_\omega}, \quad (4.2)$$

where the angular brackets are defined by Eq. (2.4). The symmetry of the optical phonons is encoded in the matrix element $g_{\boldsymbol{k},0}^\gamma$. The electron-phonon coupling of the A_{1g} and B_{1g} phonons are in a first approximation given by

$$\begin{aligned} g_{\boldsymbol{k},0}^{B_{1g}} &= g_{B_{1g}} (\cos k_x - \cos k_y)/2, \\ g_{\boldsymbol{k},0}^{A_{1g}} &= g_{A_{1g}} (\cos k_x + \cos k_y)/2. \end{aligned} \quad (4.3)$$

with the electron-phonon coupling constants $g_{B_{1g}}$ and $g_{A_{1g}}$. In Fig. 3 we have numerically evaluated the superconductivity-induced changes in the self-energy $\Sigma_\gamma(\omega)$ for B_{1g} and A_{1g} phonons in a $(d+s)$-wave superconductor. To estimate the size of these effects we have assumed some typical values for the phonon coupling strength g_γ that are in
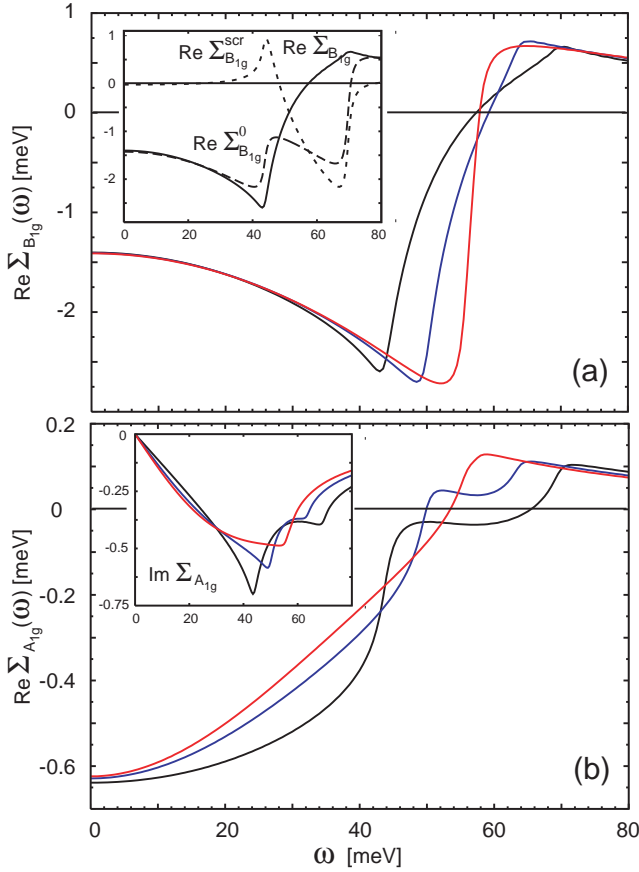
FIG. 3: (color online) Panel (a) displays the real part of the superconductivity-induced phonon self-energy $\mathrm{Re}\Sigma_{B_{1g}}(\omega)$ of the B_{1g} phonon with $g^2_{B_{1g}} = 0.1\Delta_0/N_F$ and at zero temperature according to Eq. (4.2). The fermiology parameters are the same as in Fig. 1 except for Δ_s, which varies form $\Delta_s = 0$ meV (red), to $\Delta_s = 3$ meV (blue), and $\Delta_s = 6$ meV (black). The inset shows the decomposition of the left-hand side of Eq. (4.2) into a sum of the bare contribution $\mathrm{Re}\Sigma^0_{B_{1g}}$ and the screening contribution $\mathrm{Re}\Sigma^{\mathrm{scr}}_{B_{1g}}$ when $\Delta_s = 6$ meV. Panel (b) shows the real and imaginary parts of the superconductivity-induced self-energy of the A_{1g} phonon with $g^2_{B_{1g}} = 1.0\Delta_0/N_F$ and the same fermiology parameters as in panel (a). Negative (positive) values correspond to softening (hardening) in the main frame and broadening (sharpening) in the inset of panel (b). Here N_F denotes the "normal-state" density of states per spin at the Fermi energy.

rough overall agreement with the observed Raman shifts in YBCO.[32, 33, 34, 35, 36] A negative (positive) $\mathrm{Re}\,\Sigma_\gamma(\omega)$ corresponds to a softening (hardening) of the phonon below T_c, whereas a negative (positive) $\mathrm{Im}\,\Sigma_\gamma(\omega)$ leads to a broadening (sharpening) of the phonon linewidth below T_c.

For B_{1g} phonons [see Fig. 3(a)] we find that the real part of the phonon self-energy crosses zero around $2\widetilde{\Delta}_0$ irrespective of the value of Δ_s. However, upon inclusion of a subdominant s-wave gap the maxima and minima of $\mathrm{Re}\Sigma_{B_{1g}}$ are shifted to $2(\widetilde{\Delta}_0 + \Delta_s)$ and $2(\widetilde{\Delta}_0 - \Delta_s)$, respectively. Hence, the maximal softening of the phonon frequency occurs at a

frequency $2\Delta_s$ smaller than the gap maximum $\widetilde{\Delta}_0$. The inset of Fig. 3(a) displays the decomposition of the real part of the self-energy $\mathrm{Re}\,\Sigma_{B_{1g}}(\omega)$ into its screened $\mathrm{Re}\,\Sigma^{\mathrm{scr}}_{B_{1g}}(\omega)$ and bare parts $\mathrm{Re}\,\Sigma^0_{B_{1g}}(\omega)$. The frequency dependence of these two contributions mimics that of $B^0_{1g}(\omega)$ and $B^{\mathrm{scr}}_{1g}(\omega)$, which we discussed in the previous Section. A finite s-wave component splits the step in $\mathrm{Re}\,\Sigma^0_{B_{1g}}(\omega)$ into two steps located at $2(\widetilde{\Delta}_0 \mp \Delta_s)$. In between these two steps the screening contribution $B^{\mathrm{scr}}_{1g}(\omega)$ is negative, which leads to antiscreening. Neglecting the influence of a nonzero δ_0, one can infer the Kramers-Kronig transform of the curves in Fig. 2 and thereby obtain the imaginary part of the self-energy $\mathrm{Im}\,\Sigma_{B_{1g}}(\omega)$. Due to the s-wave admixture, the frequency where the maximal broadening occurs is shifted from $2\widetilde{\Delta}_0$ to $2(\widetilde{\Delta}_0 - \Delta_s)$.[33]

Similar effects occur for the self-energy of A_{1g} phonons [see Fig. 3(b)]. An isotropic s-wave component splits the step in the real part $\mathrm{Re}\,\Sigma_{A_{1g}}(\omega)$ into two steps, thereby shifting the crossing point of $\mathrm{Re}\,\Sigma_{A_{1g}}(\omega)$ with the zero line to lower frequencies ($\Delta_s = 3$ meV) or to higher frequencies ($\Delta_s = 6$ meV). Contrary to B_{1g} phonons, antiscreening effects are absent in the self-energy of A_{1g} phonons.

Finally, we note that the effects on the superconductivity-induced changes of the phonon self-energy induced by an isotropic s-wave gap are again absent for a gap of pure d-wave character or for an extended s-wave admixture such as in Eq. (3.8). The effects on the phonon self-energy reported in this paper therefore constitute a fingerprint of an isotropic s-wave admixture to the pairing symmetry.

V. CONCLUSIONS

We have calculated the polarization-dependent Raman response for electrons and phonons in $(d + s)$-wave superconductors. We find that the screening terms in the B_{1g} channel lead to a softening of the B_{1g} pair-breaking peak of the order of $2\Delta_s$, i.e., twice the value of the isotropic s-wave component to the SC gap. This fact calls into question the long-standing interpretation that the B_{1g} pair-breaking peak is located at $\omega = 2\widetilde{\Delta}_0$ and thus can be directly used as a measure of the d-wave component of the SC gap when orthorhombicity is present. Secondly, we have estimated the effects of a subdominant s-wave admixture on the superconductivity-induced phonon renormalizations. These effects, although comparatively small, might serve as a fingerprint of an isotropic s-wave admixture to the pairing symmetry.

[1] See, for example, K. A. Müller, Nature (London) **377**, 133 (1995); D. J. Scalapino, Phys. Rep. **250**, 329 (1995).

[2] D. A. Wollman, D. J. Van Harlingen, W. C. Lee, D. M. Ginsberg, and A. J. Leggett, Phys. Rev. Lett. **71**, 2134 (1993).

[3] C. C. Tsuei, J. R. Kirtley, C. C. Chi, Lock See Yu-Jahnes, A. Gupta, T. Shaw, J. Z. Sun, and M. B. Ketchen, Phys. Rev. Lett. **73**, 593 (1994).

[4] J. Mesot, M. R. Norman, H. Ding, M. Randeria, J. C. Campuzano, A. Paramekanti, H. M. Fretwell, A. Kaminski, T. Takeuchi, T. Yokoya, T. Sato, T. Takahashi, T. Mochiku, and K. Kadowaki, Phys. Rev. Lett. **83**, 840 (1999).

[5] D. H. Lu, D. L. Feng, N. P. Armitage, K. M. Shen, A. Damascelli, C. Kim, F. Ronning, Z.-X. Shen, D. A. Bonn, R. Liang, W. N. Hardy, A. I. Rykov, and S. Tajima, Phys. Rev. Lett. **86**, 4370 (2001).

[6] V. Hinkov, S. Pailhes, P. Bourges, Y. Sidis, A. Ivanov, A. Kulakov, C. T. Lin, D. P. Chen, C. Bernhard, and B. Keimer, Nature (London) **430**, 650 (2004).

[7] H. J. H. Smilde, A. A. Golubov, A. Ariando, G. Rijnders, J. M. Dekkers, S. Harkema, D. H. A. Blank, H. Rogalla, and H. Hilgenkamp, Phys. Rev. Lett. **95**, 257001 (2005).

[8] J. R. Kirtley, C. C. Tsuei, Ariando, C. J. M. Verwijs, S. Harkema, and H. Hilgenkamp, Nat. Phys. **2**, 190 (2006).

[9] See, e.g., M. T. Béal-Monod and K. Maki, Europhys. Lett. **33**, 309 (1996); M. T. Béal-Monod, J. B. Bieri, and K. Maki, *ibid.* **40**, 201 (1997); E. Schachinger and J. P. Carbotte, Phys. Rev. B **60**, 12400 (1999); A. Bussmann-Holder, R. Micnas, and A. R. Bishop, Eur. Phys. J. B **37**, 345 (2004).

[10] R. Nemetschek, R. Hackl, M. Opel, R. Philipp, M. T. Béal-Monod, J. B. Bieri, K. Maki, A. Erb, and E. Walker, Eur. Phys. J. B **5**, 495 (1998).

[11] D. Einzel and I. Schürrer, J. Low Temp. Phys. **117**, 15 (1999); T. Strohm, and M. Cardona, Solid State Commun. **104**, 233 (1997).

[12] X. K. Chen, E. Altendorf, J. C. Irwin, R. Liang, and W. N. Hardy, Phys. Rev. B **48**, 10530 (1993).

[13] M. Opel, R. Nemetschek, C. Hoffmann, R. Philipp, P. F. Müller, R. Hackl, I. Tutto, A. Erb, B. Revaz, E. Walker, H. Berger, and L. Forro, Phys. Rev. B **61**, 9752 (2000).

[14] T. Devereaux and R. Hackl, Rev. Mod. Phys. **97**, 175 (2007), and references therein.

[15] T. P. Devereaux and D. Einzel, Phys. Rev. B **51**, 16336 (1995).

[16] A. P. Schnyder, D. Manske, C. Mudry, and M. Sigrist, Phys. Rev. B **73**, 224523 (2006).

[17] If the crystal is orthorhombic (D_{2h} point group), the A_{1g} and B_{1g} representations of the tetragonal space group (D_{4h} point group) become identical. To distinguish between these two Raman tensors an extra parameter is needed. Here, we are resolving this ambiguity by defining the A_{1g} and B_{1g} tensors in terms of the incoming and outgoing light polarization vectors as follows: We define $\gamma_{B_{1g}}$ by $\gamma_{(\hat{e}^O,\hat{e}^I)} = \gamma_{(\hat{x}',\hat{y}')}$ and for $\gamma_{A_{1g}}$ we choose $\gamma_{(\hat{e}^O,\hat{e}^I)} = \gamma_{(\hat{x}',\hat{x}')} - \gamma_{(\hat{x},\hat{y})}$, with the vectors $\hat{x} = \left(\begin{smallmatrix} +1 \\ 0 \end{smallmatrix}\right)$, $\hat{y} = \left(\begin{smallmatrix} 0 \\ +1 \end{smallmatrix}\right)$, $\hat{x}' = \frac{1}{\sqrt{2}}\left(\begin{smallmatrix} +1 \\ +1 \end{smallmatrix}\right)$, and $\hat{y}' = \frac{1}{\sqrt{2}}\left(\begin{smallmatrix} -1 \\ +1 \end{smallmatrix}\right)$.

[18] M. V. Klein and S. B. Dierker, Phys. Rev. B **29**, 4976 (1984).

[19] H. Monien and A. Zawadowski, Phys. Rev. B **41**, 8798 (1990).

[20] M. Krantz and M. Cardona, J. Low Temp. Phys. **99**, 205 (1995).

[21] T. Strohm and M. Cardona, Phys. Rev. B **55**, 12725 (1997).

[22] T. Tsuneto, Phys. Rev. **118**, 1029 (1960).

[23] M. C. Schabel, C. H. Park, A. Matsuura, Z. X. Shen, D. A. Bonn, X. Liang, and W. N. Hardy, Phys. Rev. B **57**, 6090 (1998); **57**, 6107 (1998).

[24] As in previous studies (Ref. 14), we find a suppression of the A_{1g} intensity compared to other channels, which is in disagreement with the observed spectra in high-T_c cuprates [see also F. Wenger and M. Käll, Phys. Rev. B **55**, 97 (1997)]. To resolve this discrepancy, it has been suggested that the peak in the A_{1g} channel may be identified with a collective mode (Refs. 26 and 27). Yet, it is still unclear whether this mode can explain the A_{1g} peak in the superconducting state. Here, we shall regard the peak intensities in each channel as additional fitting parameters in our phenomenological model.

[25] A. V. Chubukov, D. K. Morr, and G. Blumberg, Solid State Commun. **112**, 183 (1999).

[26] F. Venturini, U. Michelucci, T. P. Devereaux, and A. P. Kampf, Phys. Rev. B **62**, 15204 (2000).

[27] R. Zeyher and A. Greco, Phys. Rev. Lett. **89**, 177004 (2002).

[28] A. V. Chubukov, T. P. Devereaux, and M. V. Klein, Phys. Rev. B **73**, 094512 (2006).

[29] R. Zeyher and G. Zwicknagl, Z. Phys. B: Condes. Matter **78**, 175 (1990).

[30] E. J. Nicol, C. Jiang, and J. P. Carbotte, Phys. Rev. B **47**, 8131 (1993).

[31] T. P. Devereaux, Phys. Rev. B **50**, 10287 (1994).

[32] C. Thomsen, M. Cardona, B. Friedl, C. O. Rodriguez, I. I. Mazin, and O. K. Andersen, Solid State Commun. **75**, 219 (1990).

[33] B. Friedl, C. Thomsen, and M. Cardona, Phys. Rev. Lett. **65**, 915 (1990).

[34] M. F. Limonov, A. I. Rykov, S. Tajima, and A. Yamanaka, Phys. Rev. Lett **80**, 825 (1998); Phys. Rev. B **61**, 12412 (2000); see also T. Strohm, V. I. Belitsky, V. G. Hadjiev, and M. Cardona, Phys. Rev. Lett. **81**, 2180 (1998).

[35] A. Bock, Ann. Phys. **8**, 441 (1999).

[36] K. C. Hewitt, X. K. Chen, C. Roch, J. Chrzanowski, J. C. Irwin, E. H. Altendorf, R. Liang, D. Bonn, and W. N. Hardy, Phys. Rev. B, **69**, 064514 (2004).